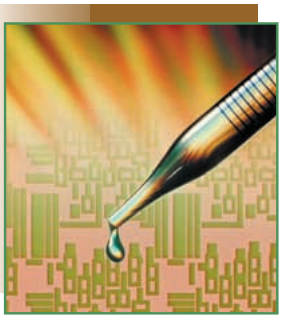



# Basic Theory of Dielectrophoresis and Electrorotation

*Methods for Determining the Forces and Torques Exerted by Nonuniform Electric Fields on Biological Particles Suspended in Aqueous Media*

THOMAS B. JONES

The forces exerted by nonuniform ac electric fields can be harnessed to move and manipulate polarizable microparticles—such as cells, marker particles, etc.—suspended in liquid media. Using rotating electric fields, controlled rotation can be induced in these same particles. The ability to manipulate suspended particles remotely without direct contact has significant potential for applications in $\mu$TAS (micro total-analysis systems) technology. The nonuniform fields for these particle manipulation and control operations are created by microelectrodes patterned on substrates using fabrication techniques borrowed from MEMS (microelectromechanical systems) technology. A wide variety of structures, ranging from simple planar geometries to complex three-dimensional (3-D) designs, are now under investigation. The implications of these various schemes in certain fields of biotechnology are far-reaching. For example, cells, cellular components, and synthetic marker particles treated with biochemical tags can be collected, separated, concentrated, and transported using microelectrode structures having dimensions of the order of 1 to 100 $\mu$m ($10^{-6}$ to $10^{-4}$ m). Furthermore, these forces can manipulate DNA particles, which are several orders of magnitude smaller than cells.

This article presents a concise, unifying treatment of the electromechanics of small particles under the influence of electroquasistatic fields and offers a set of models useful in calculating electrical forces and torques on biological particles in the size range from ~1 to ~100 $\mu$m. The theory is used to consider DEP trapping, electrorotation, traveling-wave induced motion, and orientational effects. The intent is to provide a basic framework for understanding the forces and torques exploited in the research represented by the other articles presented in this special issue of *IEEE Engineering in Medicine and Biology Magazine.*

## Effective Moment Method

The effective multipoles, including the dipole, the quadrupole, and other higher-order terms, facilitate a unified approach to electric-field-mediated force and torque calculations on particles. We first introduce the effective dipole, leaving consideration of the higher-order multipoles for later. Figure 1(a) depicts a small electric dipole of vector moment $\overline{p}^{(1)} = q\overline{d}$ located in a homogeneous, isotropic dielectric fluid of permittivity $\varepsilon_1$. The dipole experiences a nonuniform, divergence-free, electrostatic field $\overline{E}_o(\overline{r})$ imposed by electrodes not shown in the figure. To define the effective moment, it is convenient to start with the electrostatic potential due to this electric dipole [1]:

$$\Phi^{(1)} = \frac{\overline{p}^{(1)} \cdot \overline{r}}{4\pi\varepsilon_1 r^3} \tag{1}$$

where $\bar{r}$ is the radial vector distance measured from the center of the dipole and $r = |\overline{r}|$. Note the radial dependence of this potential, viz., $\Phi^{(1)} \propto r^{-2}$. If the dipole is small compared to the length scale of the nonuniformity of the imposed field $\overline{E}_o$, then the force and torque may be approximated as follows [2]:

$$\overline{F}^{(1)} \approx \left(\overline{p}^{(1)} \cdot \nabla\right)\overline{E}_o \tag{2a}$$

$$\overline{T}^{(1)} \approx \overline{p}^{(1)} \times \overline{E}_o. \tag{2b}$$

The dipole contribution to the total electric field cannot exert a force on itself and therefore is not included in $\overline{E}_o$.

Now imagine replacing the dipole by a small dielectric sphere of radius $R$ and permittivity $\varepsilon_2$ at the same position in the structure, as shown in Figure 1(b). The particle has the effect of perturbing the electric field. Expressed as an electrostatic potential, this perturbation has the form:

$$\Phi^{(1)}_{\text{induced}} \approx \frac{(\varepsilon_2 - \varepsilon_1) R^3 \overline{E}_o \cdot \overline{r}}{(\varepsilon_2 + 2\varepsilon_1) r^3} \tag{3}$$

where it has been assumed that the particle radius is small compared to the length scale of the imposed field nonuniformity. Equation (3) has the same form as (1) and the effective moment is defined by comparing these two expressions.

$$\overline{p}^{(1)}_{\text{eff}} \equiv 4\pi\varepsilon_1 K^{(1)} R^3 \overline{E}_o \tag{4}$$

where $K^{(1)} \equiv (\varepsilon_2 - \varepsilon_1)/(\varepsilon_2 + 2\varepsilon_1)$ is the Clausius-Mossotti factor. Equation (4) defines the moment of the equivalent, free-charge, electric dipole that would create a perturbation field identical to and indistinguishable from that of the dielectric sphere for all $|\overline{r}| > R$. The only distinction between this induced dipole and a general electric dipole is

 0739-5175/03/$17.00©2003IEEE 

that, because the particle is a sphere and because it is lossless, the moment will always be parallel to $\overline{E}_o$. We later take advantage of the fact that no such restriction need be imposed for force or torque calculations, thus facilitating consideration of particle inhomogeneity, anisotropy, and electrical loss.

To evaluate the force on the dielectric particle, the effective moment of (4) is substituted directly into (2a). The validity of this procedure may be argued from the standpoint of energy. An even simpler approach is to note that, if the Maxwell stress tensor is used to calculate the force, then the cases of the physical dipole and the dielectric sphere must yield the same result because, by definition, the fields are indistinguishable on any surface enclosing the particle. Combining (2a) and (4) gives the well-known expression for the DEP force on a dielectric sphere in a dielectric medium [3], [4]:

$$\overline{F}^{(1)} \equiv 2\pi R^3 \varepsilon_1 K^{(1)} \nabla E_o^2. \tag{5}$$

According to (5), a particle will be either attracted to or repelled from a region of strong electric field intensity, depending on whether $K^{(1)} > 0$ $(\varepsilon_2 > \varepsilon_1)$ or $K^{(1)} < 0$ $(\varepsilon_2 < \varepsilon_1)$, respectively. Note that combining (2b) and (4) gives zero for the torque, because the dipole moment and electric field are always parallel. To escape this restriction, the particle must be electrically lossy, nonspherical, or possess a permanent dipole moment. The lossy and nonspherical cases are considered below in the "Particle Models" and "Illustrative Cases in Biological DEP" sections, respectively.

### *Multipolar Force Contributions*

The accuracy of (5) for the DEP force depends on how particle size compares to the length scale of the nonuniformity of the imposed electric field $\overline{E}_o$. The dipole-only approximation is quite robust, and in only a few electrode geometries are multipolar correction terms needed for accurate modeling. The best example of these is a coplanar, quadrupolar electrode structure. A particle with $\varepsilon_2 < \varepsilon_1$ can be levitated passively along the centerline, where the field intensity is zero. For a particle located on the centerline, the net dipole moment is exactly zero irrespective of particle size. Thus, the particle is actually levitated by the quadrupolar force. If the particle size is increased, octupolar and other, higher-order moments can come into play [5]. Except for the planar quadrupolar electrode geometry, such a situation is unusual. In far more cases with micron-sized particles, quadrupolar corrections are negligible. Nevertheless, it is likely that, as $\mu$TAS structure sizes approach the 1-$\mu$m limit, higher-order multipolar contributions to the DEP force will become more influential for biological particles.

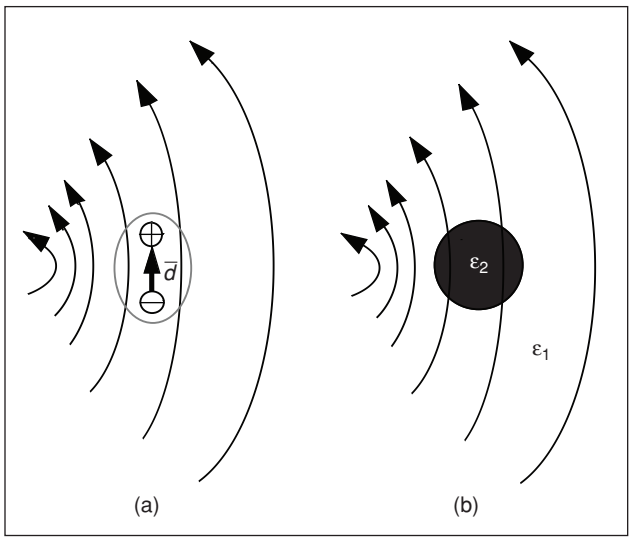


**Fig. 1.** Definition of the effective dipole moment: (a) small physical dipole in nonuniform electric field; (b) dielectric particle in the same nonuniform electric field. Assuming that the physical scale of the nonuniformity of the imposed field is much larger than the particle radius *R*, (4) may be used to evaluate the effective moment for the dielectric sphere.

Appendix A summarizes a dyadic tensor formulation for the general multipoles. In just the same way that the effective dipole moment is identified by comparing the induced electrostatic potential due to a particle in an approximately uniform electric field to the electrostatic potential of a physical dipole, one may establish the induced multipoles [6]. For the dielectric sphere shown in Figure 1(b), the general, induced tensor moment of order $n$ is

$$\overline{\overline{\overline{p}}}^{(n)} = \frac{4\pi\varepsilon_1 R^{2n+1} n}{(2n-1)!!} K^{(n)} (\nabla)^{n-1} \overline{E}_o. \tag{6}$$

In (6), $(2n-1)!! \equiv (2n-1)\cdot(2n-3)\cdot\ldots\cdot 5\cdot 3\cdot 1$, $(\nabla)^{n-1}\overline{E}$ represents $n-1$ del operations performed on the vector field, and $K^{(n)} \equiv (\varepsilon_2 - \varepsilon_1)/[n\varepsilon_2 + (n+1)\varepsilon_1]$ is the generalized Clausius–Mossotti factor. The quadrupole and all higher-order moments ($n \geq 2$) are tensors induced by spatial derivatives of $\overline{E}_o$. Note that, in a uniform field, only the dipole moment ($n = 1$) survives. Combining (6) with (A1) gives a vector expression for the $n$th multipolar contribution to the force on a dielectric sphere.

$$\overline{F}^{(n)} = \frac{4\pi\varepsilon_1 R^{2n+1}}{(n-1)!(2n-1)!!} K^{(n)} (\nabla)^{n-1} \overline{E}\,[\cdot]^n\ (\nabla)^n\, \overline{E}. \tag{7}$$

In (7), the dyadic operation $[\bullet]^n$ means $n$ dot multiplications [7]. An indicial notation provides a form often more useful for analysis. The first three terms of the $x_i$-directed component of the total force vector on a dielectric sphere are written below [6].

$$(F_{\text{total}})_i = 4\pi\varepsilon_1 R^3 \left\{ K^{(1)} E_m \frac{\partial E_i}{\partial x_m} + \frac{K^{(2)} R^2}{3} \frac{\partial E_n}{\partial x_m} \frac{\partial^2 E_i}{\partial x_n \partial x_m} + \frac{K^{(3)} R^4}{30} \frac{\partial^2 E_n}{\partial x_l \partial x_m} \frac{\partial^3 E_i}{\partial x_n \partial x_m \partial x_l} + \cdots \right\}. \tag{8}$$

Equation (8) uses the Einstein summation convention, according to which all repeated indices are summed. The first term in this expression is the same as (5), the dipolar DEP force. The second term, the quadrupole ($n = 2$), can be interpreted as the attraction of the particle to the region where the *gradient* of the electric field is highest. To make use of these expressions, it is best to consider specific classes of electrode geometries, which is a task taken up in the "Illustrative Cases in Biological DEP" section.

## Particle Models

Advantages of the effective moment method to determine force and torque start to accrue when we seek realistic models for cells and other biological particles, such as concentric shells and conductive or dielectric loss mechanisms.

### *Spherical Shells*

Biological particles are complex, heterogeneous structures with multiple layers, each possessing distinct electrical properties. Reliable dielectric models for such particles are crucial in biological dielectrophoresis. Consider the concentric, dielectric shell subjected to an electric field $\overline{E}_o$ in Figure 2(a). As before, assume that the nonuniformity of this field is modest on the scale of the particle's dimensions. It may be shown that the induced electrostatic potential outside the particle, that is, $|\overline{r}| > R_1$, is indistinguishable from that of the equivalent, homogeneous sphere of radius $R_1$ with permittivity $\varepsilon_2'$ shown in Figure 2(b) [4], if

$$\varepsilon_2' = \varepsilon_2 \left\{ \left[ \left( \frac{R_1}{R_2} \right)^3 + 2 \left( \frac{\varepsilon_3 - \varepsilon_2}{\varepsilon_3 + 2\varepsilon_2} \right) \right] \Big/ \left[ \left( \frac{R_1}{R_2} \right)^3 - \left( \frac{\varepsilon_3 - \varepsilon_2}{\varepsilon_3 + 2\varepsilon_2} \right) \right] \right\}. \tag{9}$$

In the limit of a thin shell, i.e., $(R_1 - R_2)/R_1 \ll 1$, (9) reduces to Maxwell's mixture formula [8]. The identification procedure for the effective permittivity $\varepsilon_2'$ is the same one used to identify the effective dipole moment, viz., an examination of the external induced electrostatic potential function. The effective, induced moment of the dielectric shell in Figure 2(a) is obtained by substituting $\varepsilon_2 \to \varepsilon_2'$ into the Clausius–Mossotti factor, in other words, $K^{(1)} \to (\varepsilon_2' - \varepsilon_1)/(\varepsilon_2' + 2\varepsilon_1)$.

For a general multilayered shell, the procedure is to start with the innermost sphere and the layer enclosing it, and to define an effective permittivity using (9). The procedure is then repeated on the new, now homogeneous particle and the layer enclosing it. The same step is repeated until the outermost shell has been incorporated into the effective permittivity. The particle is thus replaced by an equivalent, homogeneous sphere with a radius equal to that of the outermost shell. Strictly speaking, it is not correct to use the above effective permittivity for the higher-order moments. In the case of an electric field with significant nonuniformity, (9) can not be substituted into $K^{(2)}, K^{(3)}$, etc., because the effective permittivity differs for each multipolar moment.

### *Conductive Particles*

Accurate models for viable, biological cells suspended in media must account for ionic charge conduction mechanisms within and without the cell and, for frequencies above $\sim 1$ MHz, dielectric losses. The simplest way to represent ionic charge transport is to employ an ohmic model. Largely because of their structure and because of the high internal, electrical conductivity, this approximation usually suffices *within the cell*. On the other hand, an ohmic model is less successful in representing the aqueous, electrolytic media in which cells are commonly suspended. The problem is that double-layer phenomena introduce the complication of mobile space charge outside but directly adjacent to the cell wall [9].

In biological DEP, electrical losses manifest themselves in terms of dramatic frequency dependence of force and torque; thus, we assume sinusoidal time variation for the nonuniform electric field imposed by the electrodes:

$$\overline{E}_o(\overline{r}, t) = \mathrm{Re}\left[\underline{\overline{E}}_o(\overline{r}) \exp(j\omega t)\right] \tag{10}$$

where $\underline{\overline{E}}_o(\overline{r})$ is a spatially dependent, rms electric field vector phasor, $j = \sqrt{-1}$, $\omega$ is radian frequency, and $t$ is time. Equation (10) accommodates any type of spatially varying, ac electric field, including linearly polarized, rotating (circularly or elliptically polarized), and traveling-wave fields. Assume that both the suspension medium and the particle are homogeneous dielectrics with ohmic electrical conductivities $\sigma_1$ and $\sigma_2$, respectively. The method previously used to identify the effective dipole can be employed again, this time using phasor quantities and the following substitutions:

$$\varepsilon_1 \to \underline{\varepsilon}_1 = \varepsilon_1 + \sigma_1/j\omega \quad \text{and}$$
$$\varepsilon_2 \to \underline{\varepsilon}_2 = \varepsilon_2 + \sigma_2/j\omega. \tag{11}$$

The effective dipole moment, a vector phasor, becomes

$$\underline{\overline{p}}_{\mathrm{eff}}^{(1)} \equiv 4\pi\varepsilon_1 \underline{K}^{(1)} R^3 \underline{\overline{E}}_o. \tag{12}$$

The multiplicative factor in (12) is $\varepsilon_1$, not $\underline{\varepsilon}_1$.

The complex, frequency-dependent Clausius–Mossotti factor fits the Debye relaxation form:

$$\underline{K}^{(1)} \equiv \frac{(\underline{\varepsilon}_2 - \underline{\varepsilon}_1)}{(\underline{\varepsilon}_2 + 2\underline{\varepsilon}_1)} = K_\infty^{(1)} + \frac{K_o^{(1)} - K_\infty^{(1)}}{j\omega\tau_{\mathrm{MW}}^{(1)} + 1} \tag{13}$$

where

$$K_\infty^{(1)} \equiv (\varepsilon_2 - \varepsilon_1)/(\varepsilon_2 + 2\varepsilon_1) \quad \text{and}$$
$$K_o^{(1)} \equiv (\sigma_2 - \sigma_1)/(\sigma_2 + 2\sigma_1) \tag{14a}$$
$$\tau_{\mathrm{MW}}^{(1)} \equiv (\varepsilon_2 + 2\varepsilon_1)/(\sigma_2 + 2\sigma_1) \tag{14b}$$

$\tau_{\mathrm{MW}}^{(1)}$ is the dipolar Maxwell-Wagner relaxation time for an ohmic, dielectric sphere suspended in a similar medium. Figures 3(a) and (b) contain typical plots of $\mathrm{Re}[\underline{K}^{(1)}]$ and

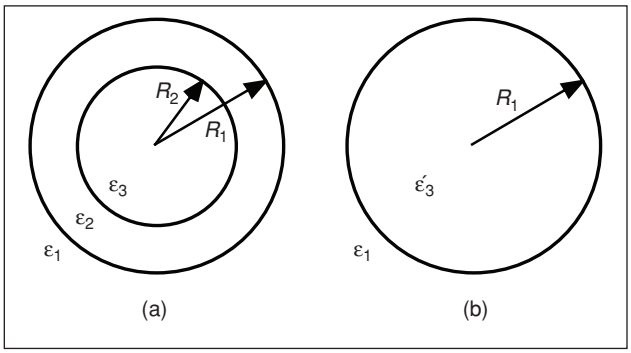


**Fig. 2.** Multilayered shells: (a) spherical particle with one concentric shell; (b) equivalent homogeneous particle. As long as the physical scale of the nonuniformity of the imposed field is much larger than the particle radius $R_1$, the external field of the equivalent particle is indistinguishable from that of the heterogeneous particle.

**The effective multipoles, including the dipole, the quadrupole, and other higher-order terms, facilitate a unified approach to electric-field-mediated force and torque calculations on particles.**

Im[$\underline{K}^{(1)}$] versus frequency. The rapid shift in the real part of $\underline{K}^{(1)}$ and the associated peak of the imaginary part at the relaxation frequency, $\omega_c = 1/\tau_{MW}^{(1)}$, are of great importance in frequency-based dielectrometry of biological cells.

The time-averaged, dipolar DEP force may now be written using (12) in (2a):

$$\langle \overline{F}^{(1)} \rangle = \mathrm{Re}\left[ \underline{\overline{p}}_{\mathrm{eff}}^{(1)} \cdot \nabla \underline{\overline{E}}_{\mathrm{o}}^{*} \right]. \tag{15}$$

Alternately, using indicial notation, the $x_i$-directed vector component of the time-average force is

$$\langle F_{\mathrm{total}} \rangle_i = 4\pi \varepsilon_1 R^3 \,\mathrm{Re}\left[ \underline{K}^{(1)} \underline{E}_m \frac{\partial \underline{E}_i^{*}}{\partial x_m} \right]. \tag{16}$$

In (15) and (16), the effective dipole moment and all electric field quantities take their rms magnitudes.

We can now reveal something of the nature of this time-average, DEP force for a completely general alternating electric field by assuming $\underline{\overline{E}} = \overline{E}_{\mathrm{R}} + \mathrm{j}\overline{E}_{\mathrm{I}}$. This form highlights the possibility that the electric field is circularly or elliptically polarized. Substituting into (15), one gets

$$\langle \overline{F}^{(1)} \rangle = 2\pi \varepsilon_1 R^3 \Big\{ \mathrm{Re}\left[ \underline{K}^{(1)} \right] \nabla E_{\mathrm{o}}^2 + 2\mathrm{Im}\left[ \underline{K}^{(1)} \right] \nabla \times \left( \overline{E}_{\mathrm{I}} \times \overline{E}_{\mathrm{R}} \right) \Big\} \tag{17}$$

where $E_{\mathrm{o}}^2 \equiv \underline{\overline{E}}_{\mathrm{o}} \cdot \underline{\overline{E}}_{\mathrm{o}}^{*}$. The first term in (17) looks just like (5) and signifies that a particle will be attracted to or repelled from regions of stronger electric field, depending on whether $\mathrm{Re}[\underline{K}^{(1)}] > 0$ or $\mathrm{Re}[\underline{K}^{(1)}] < 0$, respectively. The second term in (17) is a nonconservative force that exists only if the nonuniform field is rotating [6].

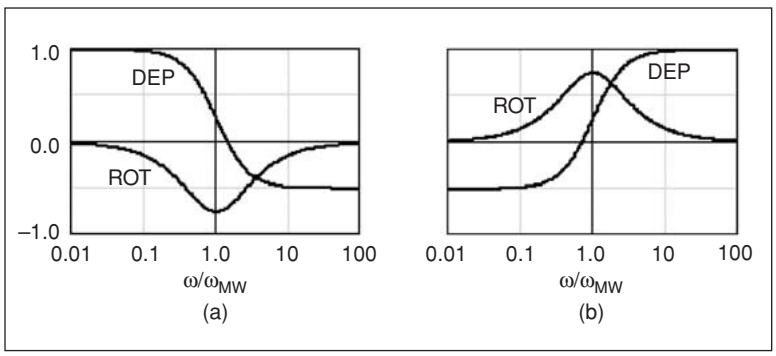


**Fig. 3.** Examples of the DEP and ROT spectra, Re($\underline{K}(\omega)$) and Im($\underline{K}(\omega)$), respectively, for two limiting cases: (a) $K_{\mathrm{o}} = 1.0$ and $K_{\infty} = -0.5$. (b) $K_{\mathrm{o}} = -0.5$ and $K_{\infty} = 1.0$. A positive or negative peak of the ROT spectrum always accompanies a change in Re($\underline{K}(\omega)$).

Combining (12) with (2b), the time average torque is

$$\langle \overline{T}^{(1)} \rangle = \mathrm{Re}\left[ \underline{\overline{p}}_{\mathrm{eff}}^{(1)} \times \underline{\overline{E}}_{\mathrm{o}}^{*} \right] = 4\pi \varepsilon_1 R^3 \,\mathrm{Re}\left[ \underline{K}^{(1)} \underline{\overline{E}}_{\mathrm{o}} \times \underline{\overline{E}}_{\mathrm{o}}^{*} \right]. \tag{18}$$

Equation (18) reveals that an electrical torque can be exerted on a sphere only if i) loss is present (i.e., the Clausius-Mossotti factor is complex) and ii) the electric field has a spatially rotating component (i.e., the field is circularly or elliptically polarized).

To incorporate dielectric loss—which is to be regarded as distinct from ohmic loss—we replace the real permittivities with complex equivalents: $\underline{\varepsilon}_1 = \varepsilon_1'(\omega) - \mathrm{j}\varepsilon_1''(\omega) + \sigma_1/\mathrm{j}\omega$ and $\underline{\varepsilon}_2 = \varepsilon_2'(\omega) - \mathrm{j}\varepsilon_2''(\omega) + \sigma_2/\mathrm{j}\omega$. Note that $\tan(\varepsilon''/\varepsilon')$ is the well-known dielectric loss tangent. When dielectric loss is incorporated in the force and torque expressions, $\varepsilon_1'$ replaces the multiplicative factor $\varepsilon_1$ appearing in (16), (17), and (18) [10], [11].

### *More About Multilayered Particles*

The introduction of loss mechanisms greatly enhances cell and bioparticle modeling capabilities. For example, (9) for the effective permittivity of a layered particle can be modified to account for conductive loss using the substitution of (11).

$$\underline{\varepsilon}_2' = \underline{\varepsilon}_2 \left\{ \left[ \left( \frac{R_1}{R_2} \right)^3 + 2\left( \frac{\underline{\varepsilon}_3 - \underline{\varepsilon}_2}{\underline{\varepsilon}_3 + 2\underline{\varepsilon}_2} \right) \right] \Big/ \left[ \left( \frac{R_1}{R_2} \right)^3 - \left( \frac{\underline{\varepsilon}_3 - \underline{\varepsilon}_2}{\underline{\varepsilon}_3 + 2\underline{\varepsilon}_2} \right) \right] \right\}. \tag{19}$$

It is not useful to attempt to extract effective conductivity and permittivity expressions from (19). Rather, the best way to understand this expression is to recognize that it adds a new Maxwell-Wagner interfacial charge relaxation mechanism to $\underline{K}(\omega)$ of the same form as (13) [12]. In general, there will be one new relaxation frequency added for each layer. Refer to Appendix E of Jones [4].

### *Particles with Thin Shells*

Particles with thin, conductive, or insulative shells serve as useful models for some of the most important dielectric behavior of biological cells. Let $R_1 = R_2 + \delta$, where $\delta \ll R \equiv R_1$. If charge transport across the thin layer dominates, one may define surface capacitance, $c_{\mathrm{m}} = \varepsilon_2/\delta$, and transconductance, $g_{\mathrm{m}} = \sigma_2/\delta$. Taking proper limits of (19) for $\delta/R \ll 1$, one obtains

$$\underline{\varepsilon}_2' = \frac{\underline{c}_m R \underline{\varepsilon}_3}{\underline{c}_m R + \underline{\varepsilon}_3}, \quad \text{where} \quad \underline{c}_m \equiv c_m + g_m/j\omega. \quad (20)$$

On the other hand, if the principal mechanism of ion transport involves motion tangential to the particle surface, then we have

$$\underline{\varepsilon}_2' = \underline{\varepsilon}_3 + 2\underline{\varepsilon}_\Sigma/R, \quad \text{where}$$
$$\underline{\varepsilon}_\Sigma \equiv \varepsilon_\Sigma + \sigma_\Sigma/j\omega, \ \varepsilon_\Sigma = \delta\varepsilon_2, \quad \text{and}$$
$$\sigma_\Sigma = \delta\sigma_2. \quad (21)$$

Figure 4 provides an interpretation for (20) and (21) in terms of a circuit model for a biological cell, such as a plant protoplast. A plant protoplast consists of a cell membrane enclosing cytoplasmic fluid. The cytoplasm contains intracellular particles, which are ignored here, but can be incorporated readily into a somewhat more complex model.

Equation (20) has the form of series-connected conductances, and in Figure 4, this complex conductance is depicted as a combination of transmembrane polarization and conduction. $c_m$ is the familiar membrane capacitance, which ordinarily dominates over the transconductance $g_m$. Equation (21) has the form of parallel conductance, consisting of surface (tangential) permittivity $\varepsilon_\Sigma$, which accounts for electric-field-induced, out-of-phase motion of bound ions tangential to the cell wall or membrane, and the more familiar surface conductivity, $\sigma_\Sigma$, which accounts for in-phase, ionic motions. If surface polarization can be ignored, i.e., $\varepsilon_\Sigma \ll \sigma_\Sigma/\omega$, then further simplification results.

$$\underline{\varepsilon}_2' \equiv \varepsilon_3 + \sigma_{\text{eff}}/j\omega \quad (22)$$

where $\sigma_{\text{eff}} \equiv \sigma_3 + 2\sigma_\Sigma/R$ is the effective ohmic conductivity of an equivalent, homogeneous particle.

### *The Multipolar Terms*

It is a straightforward matter to incorporate ohmic and dielectric loss into the general, multipolar model using complex permittivities and phasors. The tensor expression for the $n$th effective moment is:

$$\underline{\overline{\overline{p}}}^{(n)} = \frac{4\pi\varepsilon_1 R^{2n+1} n}{(2n-1)!!} \underline{K}^{(n)} (\nabla)^{n-1} \underline{\overline{E}}_o \quad (23)$$

where $\underline{K}^{(n)} = (\underline{\varepsilon}_2 - \underline{\varepsilon}_1)/[n\underline{\varepsilon}_2 + (n+1)\underline{\varepsilon}_1]$. Then, time-average expressions for force and torque are:

$$\left\langle \overline{F}^{(n)} \right\rangle = \text{Re}\left[ \frac{\underline{\overline{\overline{p}}}^{(n)} [\cdot]^n (\nabla)^n \overline{\underline{E}}_o^*}{n!} \right] \quad (24a)$$

$$\left\langle \overline{T}^{(n)} \right\rangle = \text{Re}\left[ \frac{1}{(n-1)!} \left[ \underline{\overline{\overline{p}}}^{(n)} [\cdot]^{n-1} (\nabla)^{n-1} \right] \times \overline{\underline{E}}_o^* \right]. \quad (24b)$$

Refer to Appendix B, which provides expressions for the first few terms of (24a) and (24b) in less compact but more useable, indicial notation.

### Illustrative Cases in Biological DEP

DEP trapping and levitation, electrorotation, and traveling-wave particle transport exemplify important applications of dielectrophoresis in biotechnology. In this section, we apply the theory of multipolar dielectrophoresis, introducing reasonable models for the electric field to reduce (15) and (18), and their multipolar generalizations, (24a) and (24b), to useable forms in each of these cases. The approach facilitates comparison of the ordinarily dominant dipole terms to the higher-order multipolar corrections.

### *DEP Trapping and Levitation*

The most prevalent applications envisioned for biological dielectrophoresis involve selective trapping or levitation of individual cells or particles. Related schemes take the form of continuous flow or batch separation systems. Trapping and separation often rely on the frequency-dependent, dielectric responses of particles. Highly effective schemes may be realized if one subpopulation of cells to be separated expresses a positive DEP effect, that is, $\text{Re}[\underline{K}^{(1)}] > 0$, while the other exhibits a negative effect, i.e., $\text{Re}[\underline{K}^{(1)}] < 0$. In practice, the use of frequency as a control parameter offers an excellent means to achieve selective, single-pass separations.

It may be shown that the net DEP force on a particle can be expressed as the sum of the gradients of a set of electromechanical potentials $U_n$, where $n = 1, 2, 3, \ldots$ correspond to the dipole, quadrupole, octupole, etc.; that is,

$$\overline{F}_{\text{DEP}} = -\nabla[U_1 + U_2 + U_3 + \cdots] \quad (25)$$

and the potentials are related to the electrostatic potential as follows [13]:

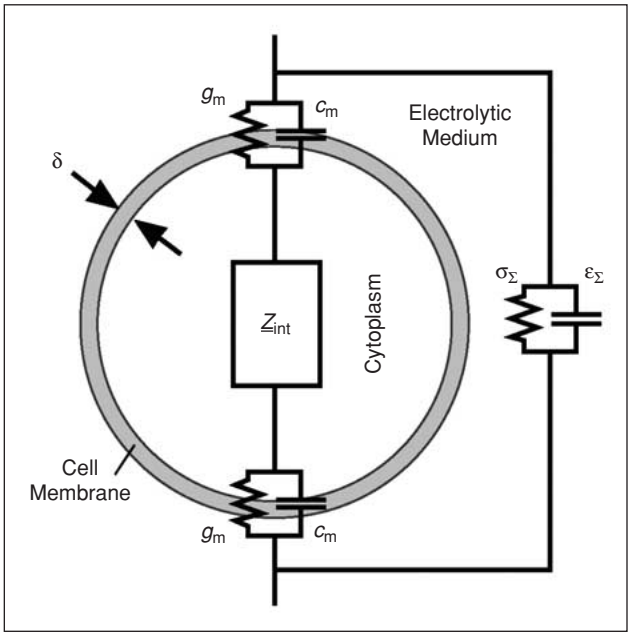


**Fig. 4.** Circuit model showing transconductance ($g_m$, $c_m$) and parallel ($g_\Sigma$, $\varepsilon_\Sigma$) paths for current flow through and around a cell. In general, both current paths exist, but usually one or the other dominates in its influence on the effective dielectric response of a particle.

$$\text{dipole:}\quad U_1 = -2\pi R^3 \varepsilon_1 K^{(1)} \left[ \left( \frac{\partial \Phi_o}{\partial x} \right)^2 + \left( \frac{\partial \Phi_o}{\partial y} \right)^2 + \left( \frac{\partial \Phi_o}{\partial z} \right)^2 \right] \tag{26a}$$

$$\begin{aligned}\text{quadrupole:}\quad U_2 = -\frac{4\pi R^5 \varepsilon_1}{3} K^{(2)} \Bigg\{ \frac{1}{2} \Bigg[ & \left( \frac{\partial^2 \Phi_o}{\partial x^2} \right)^2 + \left( \frac{\partial^2 \Phi_o}{\partial y^2} \right)^2 + \left( \frac{\partial^2 \Phi_o}{\partial z^2} \right)^2 \Bigg] \\ & + \left( \frac{\partial^2 \Phi_o}{\partial y \partial z} \right)^2 + \left( \frac{\partial^2 \Phi_o}{\partial z \partial x} \right)^2 + \left( \frac{\partial^2 \Phi_o}{\partial x \partial y} \right)^2 \Bigg\}\end{aligned} \tag{26b}$$

$$\begin{aligned}\text{octupole:}\quad U_3 = -\frac{2\pi R^7 \varepsilon_1}{5} K^{(3)} \Bigg\{ \frac{1}{6} \Bigg[ & \left( \frac{\partial^3 \Phi_o}{\partial x^3} \right)^2 + \left( \frac{\partial^3 \Phi_o}{\partial y^3} \right)^2 + \left( \frac{\partial^3 \Phi_o}{\partial z^3} \right)^2 \Bigg] \\ & + \frac{1}{2} \Bigg[ \left( \frac{\partial^3 \Phi_o}{\partial x^2 \partial y} \right)^2 + \left( \frac{\partial^3 \Phi_o}{\partial x^2 \partial z} \right)^2 + \left( \frac{\partial^3 \Phi_o}{\partial y^2 \partial x} \right)^2 + \left( \frac{\partial^3 \Phi_o}{\partial y^2 \partial z} \right)^2 \\ & + \left( \frac{\partial^3 \Phi_o}{\partial z^2 \partial x} \right)^2 + \left( \frac{\partial^3 \Phi_o}{\partial z^2 \partial y} \right)^2 \Bigg] + \left( \frac{\partial^3 \Phi_o}{\partial x \partial y \partial z} \right)^2 \Bigg\}\end{aligned} \tag{26c}$$

where $\overline{E}_o = -\nabla \Phi_o$.

Most microstructures for trapping and separation of biological particles are geometrically complicated, requiring numerical means to solve for $\Phi_o$. For purposes here, we restrict attention to azimuthally periodic structures. This class of geometries, amenable to analytical modeling, includes all cylindrically symmetric electrodes, plus many planar structures of the type commonly used to trap and rotate particles. Refer to Figure 5(a), (b), (c). The net, electrostatic potential $\Phi_o$ of all such structures may be expressed in the following series form [13]:

$$\begin{aligned}\Phi^{(m)} = V \{ & a_m + b_m z + c_m[(2m+2)z^2 - \rho^2] \\ & + d_m[(2m+2)z^3 - 3z\rho^2] + \cdots \} \rho^m \cos m\varphi\end{aligned} \tag{27}$$

where $V$ is the applied voltage and $\rho$, $\varphi$, and $z$ are cylindrical coordinates. The independent coefficients $a_m$, $b_m$, ..., are determined by the electrode geometry. The index value $m = 0$ covers the case of axisymmetric structures, while $m > 0$ accounts for axially periodic geometries, in which case $m$ can be interpreted as the number of salient electrode pairs.

If (27) is substituted into the electromechanical potential expressions, the axial and radial force component can be obtained. It is convenient to treat separately the axisymmetric ($m = 0$) and azimuthally periodic ($m > 0$) cases.

### Axisymmetric Electrodes: $m = 0$

Consider a particle in a cusped electric field as shown in Figures 5(a) or 5(b). Assume that the particle, initially in equilibrium at $z = 0$, $\rho = 0$, is displaced by some small amounts $z'$ and $\rho'$. Correct to quadrupolar terms, the axial and radial force components are:

$$\begin{aligned}F_z \approx & 16\pi \varepsilon_1 R^3 K^{(1)} \left[ b_o c_o + \left( 4c_o^2 + 3b_o d_o \right) z' \right] V^2 \\ & + 96\pi \varepsilon_1 R^5 K^{(2)} \left( c_o d_o + 3 d_o^2 z' \right) V^2\end{aligned} \tag{28a}$$

$$\begin{aligned}F_\rho \approx & \left[ 8\pi \varepsilon_1 R^3 K^{(1)} \left( 2c_o^2 - 3 b_o d_o \right) \right. \\ & \left. + 96\pi \varepsilon_1 R^5 K^{(2)} d_o^2 \right] \rho' V^2\end{aligned} \tag{28b}$$

(28a) and (28b) may be used to determine the equilibrium condition, i.e., the voltage-dependent levitation position, and, just as important, the stability of the equilibrium with respect to small displacements. It is only necessary to obtain the coefficients $b_o$, $c_o$, $d_o$, etc., via appropriate analytical or numerical means.

The relative magnitudes of the dipolar and quadrupolar terms may be compared using

$$\frac{F_{\text{quad}}}{F_{\text{dipole}}} = \frac{96\pi R^5 K^{(2)} c_0 d_0}{16\pi R^3 K^{(1)} b_0 c_0} \approx \frac{6 d_0}{b_0} R^2. \tag{29}$$

For one axisymmetric DEP levitator where the particle diameter was less than 1/10 the electrode spacing, the quadrupolar correction was estimated to be less than 1% [14]; however, the $R^2$ dependence of (29) indicates that the correction will become significant as particle size is increased [5].

### Azimuthally Periodic Electrodes: $m > 0$

For azimuthally periodic structures, it is convenient to select a specific value for $m$. Consider the 4-pole structure shown in Figure 5(c), for which $m = 2$. The force terms are:

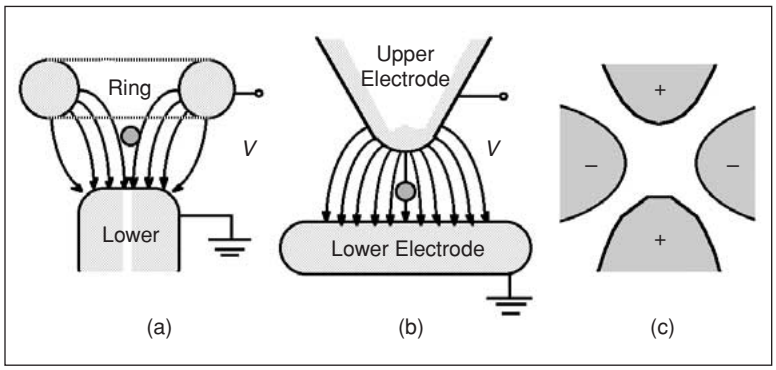


**Fig. 5.** Some representative trapping and levitation electrode structures. (a) Side view of cusped electric field for negative DEP levitation ($m = 0$); (b) side view of electric field for positive DEP levitation ($m = 0$); (c) top view of azimuthally periodic electrodes for quadrupolar electric field ($m = 2$) with zero field magnitude along the central axis.

**Advantages of the effective moment method to determine force and torquestart to accrue when we seek realistic models for cells and other biological particles.**

$$F_z \approx \frac{32}{3}\pi\varepsilon_1 R^3 K^{(2)}\left[a_2 b_2 + \left(b_2^2 + 12a_2c_2\right)z'\right] V^2 \quad (30a)$$

$$F_\rho \approx 16\pi\varepsilon_1\left[R^3K^{(1)}a_2^2 + \frac{2}{3}R^5K^{(2)}\left(b_2^2 - 6a_2c_2\right)\right]\rho' V^2 \quad (30b)$$

Because the electric field is zero on the axis, there is no net induced dipole so the axial levitation force is provided by the quadrupolar term [5]. On the other hand, the radial restoring force term (proportional to $\rho'$) contains both dipolar and quadrupolar contributions. Just as for the $m = 0$ case, one may investigate equilibria and their stability from (30a) and (30b), if the coefficients $a_2$, $b_2$, and $c_2$ are known.

### *Electrorotation*

The electrode structure of Figure 6 can be excited with multiphase ac voltage to create a rotating electric field. If the field rotates counter-clockwise, it will have the following vector phasor form on the axis:

$$\overline{\underline{E}}(x, y) = E_0(\hat{x} - \mathrm{j}\hat{y}) \quad (31)$$

where $\hat{x}$ and $\hat{y}$ are orthogonal unit vectors. If a spherical particle is introduced at the center, its induced dipole moment is

$$\overline{\underline{p}}_{\text{eff}} = 4\pi\varepsilon_1 R^3 \underline{K}^{(1)} E_0(\hat{x} - \mathrm{j}\hat{y}) \quad (32)$$

This dipole moment rotates in synchronism with the electric field but lags behind it by a phase factor associated with the complex, frequency-dependent Clausius-Mossotti factor, $\underline{K}^{(1)}$. It is this phase factor that makes electrorotation possible. From (18), the time-average electrorotational torque is:

$$\left\langle \overline{T}^{(1)} \right\rangle = -4\pi\varepsilon_1 R^3 \,\mathrm{Im}\left[\underline{K}^{(1)}(\omega)\right] E_{\text{o}}^2. \quad (33)$$

Note that the torque depends on the imaginary part of $\underline{K}^{(1)}$, which is nonzero only if there is a loss mechanism.

For a homogeneous sphere with complex permittivity $\underline{\varepsilon}_2 = \varepsilon_2 + \sigma_2/\mathrm{j}\omega$ in a fluid with $\underline{\varepsilon}_1 = \varepsilon_1 + \sigma_1/\mathrm{j}\omega$, the time-average torque is:

$$\left\langle \overline{T}^{(1)} \right\rangle = -\frac{6\pi\varepsilon_1 R^3 E_{\text{o}}^2 (1 - \tau_1/\tau_2)\omega\tau_{\text{MW}}}{(1 + 2\varepsilon_1/\varepsilon_2)(1 + \sigma_2/2\sigma_1)[1 + (\omega\tau_{\text{MW}})^2]} \quad (34)$$

where $\tau_1 = \varepsilon_1/\sigma_1$, $\tau_2 = \varepsilon_2/\sigma_2$, and $\tau_{\text{MW}} = \tau_{\text{MW}}^1$ from (14b). As shown in Figures 3(a) and 3(b), the torque exhibits a peak at $\omega = \tau_{\text{MW}}^{-1}$ and the sign of this peak is positive or negative, depending on the relative magnitudes of $\tau_1$ and $\tau_2$. The possibility of positive or negative torque means that the particle can rotate, respectively, with the electric field or in the opposite direction. Note that $\overline{\underline{p}}_{\text{eff}}$ always rotates with the electric field. Refer to Jones for a physical interpretation of these distinct cases [4].

The rotation of particles with multiple layers can be modeled by substituting the effective complex permittivity of (19) into (13). Particles with multiple layers usually display multiple peaks, each of which reveals useful information.

### *Traveling-Wave DEP*

Consider the planar, horizontal electrode array shown in Figure 7. If these electrodes are driven by polyphase ac, a traveling wave of electrostatic potential is created that can suspend a lossy dielectric sphere vertically while simultaneously propelling it along the array. To first order, the electric field may be represented by a simple harmonic wave traveling from left to right. A convenient phasor form for the Laplacian electric field is

$$\overline{\underline{E}}(x, y) = E_0(\mathrm{j}\hat{x} + \hat{y})\exp(-\mathrm{j}kx - ky) \quad (35)$$

where $k = 2\pi/\lambda$ is the wavenumber and $\lambda$ is the wavelength imposed by the center-to-center electrode spacing plus the electrical phasing. Note that, at any fixed point, the electric field polarization is circular and counterclockwise. A lossy particle suspended above these electrodes will experience simultaneously x- and y-directed dielectrophoretic forces, as well as a torque.

Using (35) in (B1) and (B2) for the $x$- and $y$-directed components of the time-average DEP force, we obtain

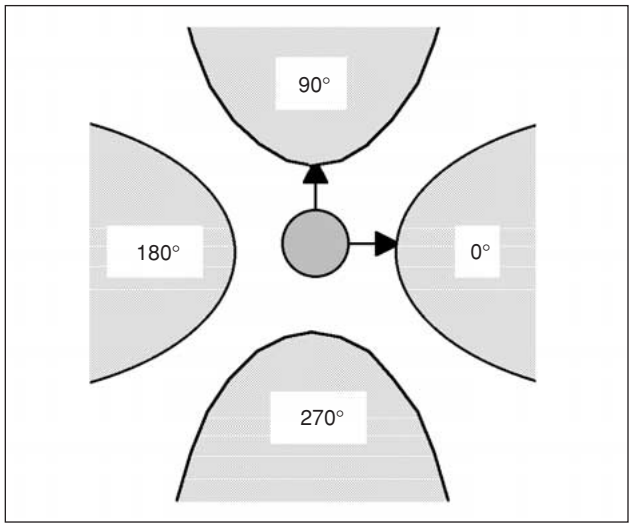


**Fig. 6.** Four-pole electrode structure to create a rotating electric field showing the phasing of the voltage excitation.

$$\langle F_x \rangle = -4\pi\varepsilon_1 R^3 k E_0^2 \exp(-2ky) \times \left[ \mathrm{Im}\left[\underline{K}^{(1)}\right] + \frac{2k^2R^2}{3}\mathrm{Im}\left[\underline{K}^{(2)}\right] + \cdots \right] \quad (36a)$$

$$\langle F_y \rangle = -4\pi\varepsilon_1 R^3 k E_0^2 \exp(-2ky) \times \left[ \mathrm{Re}\left[\underline{K}^{(1)}\right] + \frac{2k^2R^2}{3}\mathrm{Re}\left[\underline{K}^{(2)}\right] + \cdots \right] \quad (36b)$$

which is correct to the quadrupolar term. Note that the $x$-directed, *translational* force depends on the imaginary parts of the complex polarization coefficients. This force propels the particle in the $+x$ or $-x$ direction depending whether $\mathrm{Im}[\underline{K}^{(1)}]$ is negative or positive, respectively. The $y$-directed force will either levitate the particle above the electrodes or hold it down against them, depending on whether $\mathrm{Re}[\underline{K}^{(1)}]$ is negative or positive, again respectively. The quadrupolar corrections in (36a) and (36b) becomes comparable to the dipolar term when $R \approx 0.19\lambda$.

Using (35) in (B4) and (B5) gives the time-average torque for a particle in the traveling wave structure.

$$\langle T_z \rangle = -4\pi\varepsilon_1 R^3 E_0^2 \exp(-2ky) \times \left[ \mathrm{Im}\left[\underline{K}^{(1)}\right] + \frac{4k^2R^2}{3}\mathrm{Im}\left[\underline{K}^{(2)}\right] + \cdots \right]. \quad (37)$$

Comparing (36a) and (36b) to (37), we see that the quadrupole correction is more influential for the electrorotational torque than for the DEP force. It should be pointed out that $\underline{K}^{(2)}$ has almost the same Maxwell–Wagner relaxation frequency as $\underline{K}^{(1)}$. As a result, the effect of the quadrupole terms in (36a), (36b), and (37) is to increase the magnitudes of the force and torque spectra but not significantly to alter the frequency dependence.

This analysis has been performed for a simple, harmonic, traveling electric field wave, with the electric field confined to two dimensions. Superposition may be employed to evaluate forces and torques using (36a), (36b), and (37) for any electrode geometry, with the electric field obtained by analytical or numerical means. Numerical methods are in fact essential if one wishes to account for the finite size of segmented electrodes in real structures.

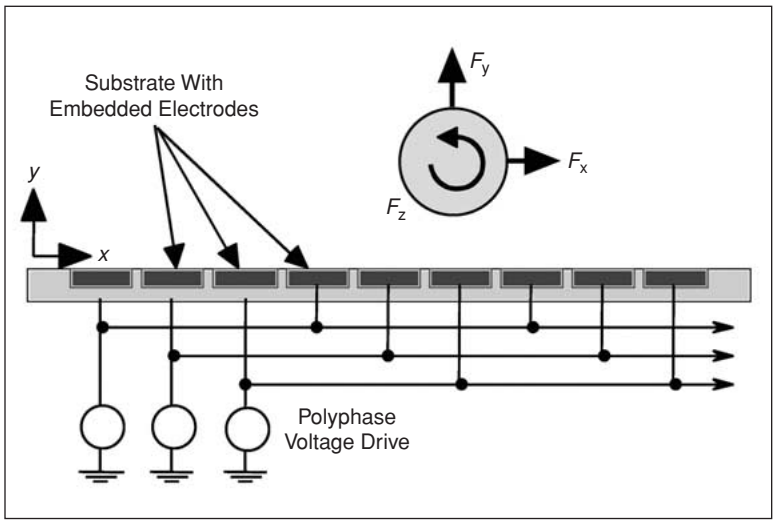


**Fig. 7.** Traveling wave electrode structure. The traveling wave electric field suspends the particle above the plane of the electrodes if $\mathrm{Re}(\underline{K}(\omega)) < 0$. The induced motion is left to right or right to left depending on whether $\mathrm{Im}(\underline{K}(\omega)) < 0$ or $\mathrm{Im}(\underline{K}(\omega)) > 0$. In addition, the particle will rotate as it moves along.

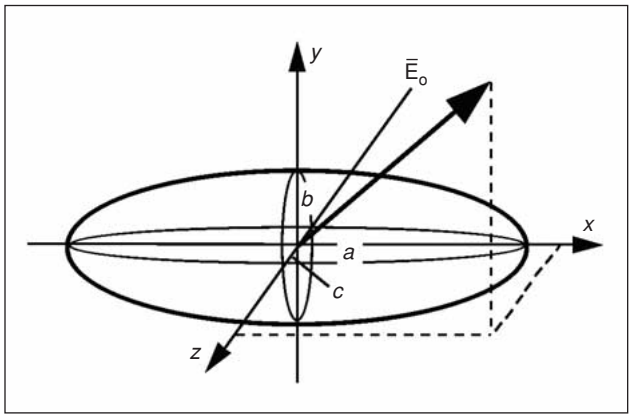


**Fig. 8.** A spheroidal dielectric particle in a uniform electric field. The semimajor axes are $a > b > c$. The particle experiences an electrical torque that seeks to align the particle with any of the axes, but only alignment along the longest axis ($a$) is stable.

## Alignment of Nonspherical Particles

Nonspherical shapes are far more common forms of bioparticles than spheres. The most important cells in biomedical science are mammalian erythrocytes (red blood cells). Human erythrocytes are essentially oblate spheroids with one side indented, while those of certain ruminants, e.g., the llama, happen to be fairly close to ideal spheroids with the three semi-major axes in the approximate ratio of 4:2:1 [15]. Nonspherical shape imparts geometric anisotropy to a particle, with the result that the induced dipole moment is parallel to the imposed electric field only if the particle is aligned with one of its principal axes parallel to the field. Refer to Figure 9. As a result, such particles experience an alignment torque in a uniform electric field.

The effective moment of a homogeneous spheroid having semi-major axes $a$, $b$, and $c$ may be written [1]:

$$\bar{p}_{\mathrm{eff}} = \frac{4\pi abc}{3}(\varepsilon_2 - \varepsilon_1)\bar{E}^- \quad (38)$$

where $\bar{E}^-$ is the uniform electric field internal to the particle, which, in general, is not parallel to $\bar{E}_o$.

$$E_x^- = E_{o,x}/[1 + (\varepsilon_2 - \varepsilon_1)L_x/\varepsilon_1], \text{ where}$$
$$L_x \equiv \frac{abc}{2}\int_0^\infty \frac{ds}{(s+a^2)R_s} \quad (39)$$

where $R_s \equiv \sqrt{(s+a^2)\,(s+b^2)\,(s+c^2)}$. Similar expressions for the $y$ and $z$ components of the internal field are readily ascertained from (39). To determine the DEP force and torque on the ellipsoid, the effective moment from (38) is substituted into (2a) and (2b), respectively.

Of interest here is the torque, the $x$ component of which is

$$T_x^{\mathrm{e}} = \frac{4\pi abc(\varepsilon_2 - \varepsilon_1)^2 (L_z - L_y) E_{o,y} E_{o,z}}{3\varepsilon_1 \left[1 + \left(\frac{\varepsilon_2 - \varepsilon_1}{\varepsilon_1}\right) L_y\right] \left[1 + \left(\frac{\varepsilon_2 - \varepsilon_1}{\varepsilon_1}\right) L_z\right]}. \tag{40}$$

With no loss of generality, we may assume that the electric field components are all positive and that $a > b > c$, in which case $0 < L_x < L_y < L_z < 1$. Thus, $T_x^{\mathrm{e}} < 0, T_y^{\mathrm{e}} > 0$, and $T_z^{\mathrm{e}} > 0$, which means that the electrical torque always tends to align the particle with one of its axes parallel to the electric field. Only one of these alignments, viz., the one where the longest axis is parallel to the field, is stable. Prolate and oblate spheroids are readily treated as special cases [4].

For a lossy ellipsoid, alignment and stability assume a frequency-dependent aspect. It is no longer true that only the longest axis is stable. In fact, depending on relative conductivity and permittivity values, all three orientations become possible, each in a different frequency range. The stable orientation in the low- and high-frequency limits is always with the long axis parallel to the field, but for intermediate values, a particle will flip spontaneously to new orientation as each of several critical frequencies is reached. The set of turnover frequencies is called the orientational spectrum [15], and the cause of this behavior is the distinct Maxwell-Wagner charge relaxation time constants for each of the three orientations. Ellipsoids with multiple layers can be treated in a way analogous to the method explicated in above; however, there arises the difficulty that the effective complex permittivity is different for each axis.

## Conclusion

In this article, the effective dipole method, and its generalization to effective multipoles, has been exploited to evaluate forces and torques exerted on small particles by electric fields. The method makes it possible to treat multilayered concentric shells and particles exhibiting ohmic and dielectric loss. This method may be extended further to the case of nonspherical particles, where alignment torques can be considered. These capabilities are well suited to modeling DEP behavior of biological particles including cells.

The models and methods presented in this review are sufficiently general to be of use in a broad range of applications for biological dielectrophoresis and particle electrokinetics. The range of validity can be stated confidently to cover particles having diameters approximately 1 $\mu$m and larger. However, advances in fabrication techniques for nanostructures coupled with ever-increasing demands for new capabilities for manipulation and detection of biomolecules are inexorably pushing particle size limits downward into the nanometer range. While the scaling laws of DEP and electrorotation would suggest that electrostatic forces should become more and more dominant as size is reduced below 1 $\mu$m [16], it is well to bear in mind that other forces, usually ignored for a 10-$\mu$m particle , become influential for a 100-nm particle. Furthermore, the discernible size scale of distributed electrical charges in proteins starts at $\sim 10^2$ nanometer. The implication of such charge distributions for the electrical forces and torques is that the higher-order multipoles, usually small corrections for a 10-$\mu$m particle, may become dominant in biomolecules. The lesson of these observations is that the simple models reviewed in this article will require modification and correction as biotechnology moves into the nanoscale.


## Acknowledgments

The author has benefited from research collaborations extending over many years with K.V.I.S. Kaler at the University of Calgary and M. Washizu at Tokyo University. He is pleased to acknowledge past financial support from the Eastman Kodak Company, the National Science Foundation, and the Japan Society for the Promotion of Science.



**Thomas B. Jones** received the Ph.D. degree in electrical engineering from the Massachusetts Institute of Technology, Cambridge, in 1970. He began his professional career in 1970 at Colorado State University in Ft. Collins, where he taught and did research for 11 years. In 1981, he joined the technical staff at Xerox Corporation in Webster, New York, to conduct research on xerographic physics. In 1984, he left Xerox to become professor of electrical engineering at the University of Rochester. He focused his research for many years on the behavior of small particles in electric and magnetic fields, and in 1995, he authored the monograph Electromechanics of Particles. His present interests are in the exploitation of electrical forces to microfluidics systems for application in the laboratory on a chip. He was a member of the Electrostatic Processes Committee of the IAS for many years and served as chair from 1985 to 1987. From 1996 to 1999, he was a member of the IAS/IEEE Fellow Nominating Committee and served as chair during the last year. Prof. Jones was editor-in-chief of the Journal of Electrostatics from 1992 to 2003. He has consulted extensively in industrial electrostatic hazards and nuisances and co authored a book on that subject titled Powder Handling and Electrostatics in 1991.

**Address for Correspondence:** T.B. Jones, Department of Electrical and Computer Engineering, University of Rochester, Rochester, NY 14627 USA. E-mail: jones@ece.rochester.edu.


## References


[1] J.A. Stratton, *Electromagnetic Theory*. New York: McGraw-Hill, 1941, section 3.9.
[2] P. Lorrain and D.R. Corson, *Electromagnetic Fields and Waves,* 2nd ed.. San Francisco, CA: W.H. Freeman, 1970, section 3.12.
[3] H.A. Pohl, *Dielectrophoresis*. Cambridge, UK: Cambridge University Press, 1978.
[4] T.B. Jones, *Electromechanics of Particles*. New York: Cambridge University Press, 1995.
[5] T. Schnelle, T. Müller, and G. Fuhr, "Manipulation of particles, cells, and liquid droplets by high frequency electric fields," *Biomethods*, vol. 10, pp. 417–452, 1999.
[6] T.B. Jones and M. Washizu, "Multipolar dielectrophoretic and electrorotational theory," *J. Electrostatics*, vol. 37, pp. 121–134, 1996.
[7] R.B. Bird, R.C. Armstrong, and O. Hassager, *Dynamics of Polymeric Liquids: Fluid Mechanics* (vol. 1). New York: Wiley, 1977.
[8] J.C. Maxwell, *A Treatise on Electricity and Magnetism*, New York: Dover Press, 1954, art. 314.
[9] G. Schwarz, "A theory of the low-frequency dielectric dispersion of colloidal particles in electrolyte solution," *J. Chem. Phys.*, vol. 66, pp. 2636–2642, 1962.
[10] F.A. Sauer, "Interactions forces between microscopic particles in an external electromagnetic field," in *Interactions Between Electromagnetic Fields and Cells*, A. Chiabrera, C. Nicolini, and H.P. Schwan, Eds. New York: Plenum, 1985, pp. 181–202.
[11] F.A. Sauer and R.W. Schlögel, "Torques exerted on cylinders and spheres by external electromagnetic fields," in *Interactions Between Electromagnetic Fields and Cells*, A. Chiabrera, C. Nicolini, and H.P. Schwan, Eds. New York: Plenum, 1985, pp. 203–251.
[12] X-B. Wang, R. Pethig, and T.B. Jones, "Relationship of dielectrophoresis and electrorotational behavior exhibited by polarized particles," *J. Phys. D: Appl. Phys.*, vol. 25, pp. 905–912, 1992.
[13] T.B. Jones and M. Washizu, "Equilibria and dynamics of DEP-levitated particles: multipolar theory," *J. Electrostatics*, vol. 33, pp. 199–212, 1994.
[14] T.B. Jones, "Multipole corrections to dielectrophoretic force," *IEEE Trans.*

*Industry Applicat.,* vol. IA-21, pp. 930–934, 1985.
[15] R.D. Miller and T.B. Jones, "Electro-orientation of ellipsoidal erythrocytes: Theory and experiment," *Biophys. J.*, vol. 64, pp. 1588–1595, 1993.
[16] T.B. Jones, "Electrostatics on the Microscale," presented at *Electrostatics 2003*, Institute of Physics (UK), Edinburgh, April, 2003.
[17] C-T. Tai, *Generalized Vector and Dyadic Analysis*, New York: IEEE Press, 1992, ch. 7.

## Appendix A

Figure A1 illustrates a straightforward way to generate the general multipoles, starting with a point charge $q_o$, and then progressively moving to the dipole, quadrupole, etc. According to this construction, the dipole is formed from two opposite sign charges displaced by $\overline{d}_1$; the quadrupole is then formed from two opposite sign dipoles displaced by $\overline{d}_2$. For generality, each vector displacement must be independent. The force and torque on a multipole of order $n$ are [6]:

$$\overline{F}^{(n)} = \frac{\overline{\overline{\overline{p}}}^{(n)}[\cdot]^n(\nabla)^n\overline{E}_o}{n!} \tag{A1}$$

$$\overline{T}^{(n)} = \frac{1}{(n-1)!}\left[\overline{\overline{\overline{p}}}^{(n)}[\cdot]^{n-1}(\nabla)^{n-1}\right]\times\overline{E}_o \tag{A2}$$

and the multipoles are described in dyadic tensor form [6]

$$\overline{\overline{\overline{p}}}^{(n)} = q_n \sum_{\substack{\text{all permutations of}\\ i\neq j\ldots\neq k \text{ with } 1\le i\le n,\\ 1\le j\le n,\ldots,1\le k\le n}} \overline{d}_i\overline{d}_j\ldots\overline{d}_k. \tag{A3}$$

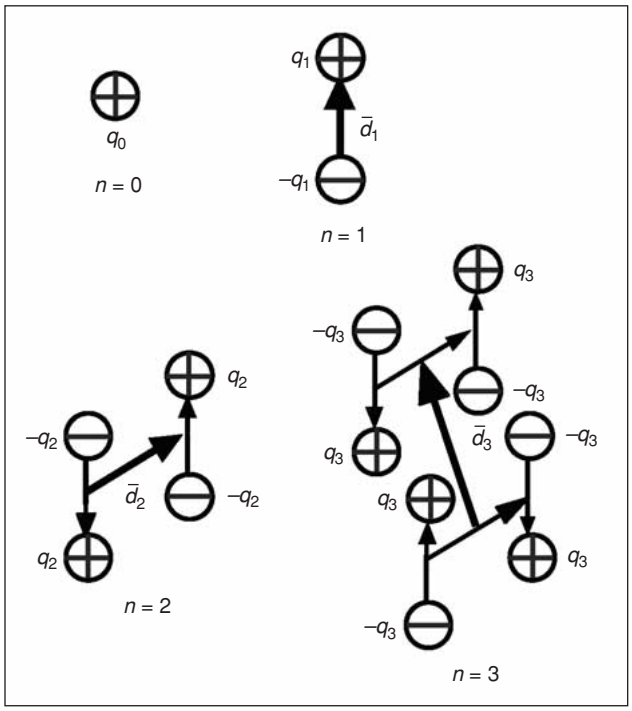


**Fig. A1.** Systematic generation of multipoles starting from a point charge. In the case of the general multipole, each displacement must be independent.

The summation in (A3) guarantees that all tensor moments are symmetric [17]. This is a requirement because force and torque cannot depend upon the order in which the displacements creating the multipole are taken. The general expression for the electrostatic potential due to the multipole of order $n$ is

$$\Phi^{(n)} = (-1)^n\frac{\overline{\overline{\overline{p}}}^{(n)}[\cdot]^n(\nabla)^n\left(\frac{1}{r}\right)}{4\pi\varepsilon_1 n!}. \tag{A4}$$

## Appendix B

Using (23), the individual force components of (24a) can be expressed in a convenient, indicial form. The $i$-directed components of the $n$ =1, 2, and 3 terms of the force are:

$$\text{dipole } (n=1): \left\langle F_i^{(1)}\right\rangle = 4\pi\varepsilon_1 R^3\ \text{Re}\left[\underline{K}^{(1)}\underline{E}_m\frac{\partial}{\partial x_m}\underline{E}_i^*\right] \tag{B1}$$

$$\text{quadrupole } (n=2): \left\langle F_i^{(2)}\right\rangle = \frac{4}{3}\pi\varepsilon_1 R^5 \times \text{Re}\left[\underline{K}^{(2)}\frac{\partial\underline{E}_n}{\partial x_m}\frac{\partial^2\underline{E}_i^*}{\partial x_n\partial x_m}\right] \tag{B2}$$

$$\text{octupole}(n=3): \left\langle F_i^{(3)}\right\rangle = \frac{2}{15}\pi\varepsilon_1 R^7 \times \text{Re}\left[\underline{K}^{(3)}\frac{\partial^2\underline{E}_n}{\partial x_l\partial x_m}\frac{\partial^3\underline{E}_i^*}{\partial x_n\partial x_m\partial x_l}\right] \tag{B3}$$

In the above, we employ the Einstein summary convention (ESC), according to which one sums over all repeated indices.

Equation (24b) for the torque also can be reduced to more convenient and easily interpreted equations in indicial form. All electric field variables take their rms magnitudes.

$$\text{dipole } (n=1): \ T_i^{(1)} = -4\pi\varepsilon_1 R^3\text{Im}\left[\underline{E}_j\underline{E}_k^*\right]\text{Im}\left[\underline{K}^{(1)}\right] \tag{B4}$$

$$\text{quadrupole } (n=2): \ \overline{T}_i^{(2)} = \frac{-8\pi\varepsilon_1 R^5}{3} \times \text{Im}\left[\frac{\partial\underline{E}_j}{\partial x_m}\frac{\partial\underline{E}_k^*}{\partial x_m}\right]\text{Im}\left[\underline{K}^{(2)}\right] \tag{B5}$$

$$\text{octupole } (n=3): \overline{T}_i^{(3)} = -\frac{2\pi\varepsilon_1 R^7}{5} \times \text{Im}\left[\frac{\partial^2\underline{E}_j}{\partial x_m\partial x_n}\frac{\partial^2\underline{E}_k^*}{\partial x_m\partial x_n}\right]\text{Im}\left[\underline{K}^{(3)}\right] \tag{B6}$$

In (B4), (B5), and (B6), indices $i$, $j$, and $k$ must be in right-hand sequence: $xyz$, $yzx$, or $zxy$. These equations share two common requirements for nonzero electrical torque: i) $\text{Im}[\underline{K}^{(n)}] \neq 0$, i.e., the particle (or the suspension medium) must be lossy, and ii) the orthogonal electric field components $\underline{E}_j$ and $\underline{E}_k$ must be out of phase, i.e., the field vector must rotate in time.